

Aeolus' Instrument Response Calibration

Uwe Marksteiner^(a), Oliver Lux^(a), Oliver Reitebuch^(a), Benjamin Witschas^(a), Jos de Kloe^(b),
Gert-Jan Marseille^(b) and Michael Rennie^(c)

^(a) DLR German Aerospace Center, Institute of Atmospheric Physics, Oberpfaffenhofen 82234 Germany

^(b) Royal Netherlands Meteorological Institute (KNMI), De Bilt, The Netherlands

^(c) European Centre for Medium-Range Weather Forecast, Reading, UK

Uwe.Marksteiner@dlr.de

Abstract: Aeolus was the first Doppler wind lidar in space. During its almost 5 years lifetime after launch in August 2018 it made use of two lasers operating at a wavelength of 354.8 nm. In contrast to coherent wind lidars that use heterodyning, the direct-detection approach applies high-resolution interferometry and hence requires accurate and regular calibration, but also allows measurements outside aerosol-loaded areas. The Instrument Response Calibration (IRC) plays an essential role in the Aeolus processing chain for L1B wind data, and helps to ensure the precision and accuracy of L2B wind data disseminated to the scientific community. The IRC is used to determine spectral characteristics of the receiver and the relationship between the instrument measurement output data (the response) and the actual frequency shift. We explain fundamental aspects of IRC, such as the monitoring of IRC-related parameters, the quality assessment of the receiver channels' calibration curves and the utilization of IRC-based parameters in the wind retrieval algorithm.

1. Introduction

After the successful launch of the Aeolus satellite on 22 August 2018, its single payload ALADIN (Atmospheric LASer Doppler INstrument), equipped with two flight model (FM) lasers FM-A and FM-B, became the first European lidar and the first Doppler Wind Lidar (DWL) in space [1-3]. From then on until the first-of-its-kind assisted reentry of Aeolus in July 2023, the instrument was operated from a polar, sun-synchronous dusk-dawn orbit at a mean altitude of 320 km with an orbit repeat cycle of 1 week.

Two measurement approaches have been found to be particularly effective for the challenging task of detecting small Doppler shifts in electromagnetic radiation: The direct-detection approach utilizing high-resolution interferometry and the coherent approach involving heterodyning.

The advantage of the latter is that a coherent Doppler wind lidar does not need a calibration describing the system's response to the return signal. However, the limitation of the coherent technique to spectrally narrow returns signals restricts its use to aerosol-loaded areas like dust layers, volcanic ash plumes or the planetary boundary layer. By using high-resolution

filters, the direct-detection technique allows for the analysis of narrowband Mie spectra, too. Here, the observed Doppler frequency shift can be associated for example with the position of an intensity maximum, e.g. an interference fringe, on a suitable detector. In addition, the use of filters enables the derivation of Doppler shifts from broadband Rayleigh spectra, to which the principle of coherent detection is not applicable. In this case, the frequency shift can be related to a change in the intensity transmitted through the filters. Consequently, one benefit of the direct-detection technique lies in its ability to analyse the molecular backscatter signal, which occurs reliably in the atmosphere at all altitudes [4]. Based on the λ^{-4} - dependence of the effective scattering cross-section of molecules, such lidar systems are advantageously operated at short wavelengths.

Therefore, ALADIN emitted laser pulses in the ultra-violet (UV) at 354.8 nm. It did so with a repetition frequency of 50.5 Hz, a linewidth of about 50 MHz, a frequency stability of mostly 7 MHz [5] and reported pulse energies varying between 40 mJ and 101 mJ during the nominal mission lifetime. The backscattered light was collected by a primary mirror with a diameter of 1.5 m and guided onto two different interferometers: a Fizeau for the Mie type signal and a Double-Fabry-Perot for the molecular

Rayleigh signal. The wind velocity measurements were performed under an off-nadir angle of 35° along the line-of-sight (LOS), obtaining only one component of the wind vector.

Aeolus uses two rectangularly arranged Accumulation Charge Coupled Devices (ACCD) with an imaging zone of 16×16 pixels. The light transmitted through the Fizeau interferometer is formed to a linear fringe which in turn is mapped onto the ACCD, with the position of the fringe being denoted as the Mie response. On the other ACCD, the light transmitted through the double Fabry-Perot interferometer forms two spots A and B, with the contrast ratio of the sum of each being denoted as Rayleigh response R_R in dependence of the laser emit frequency f :

$$R_R(f) = (A(f) - B(f)) / (A(f) + B(f)) \quad (1)$$

Several corrections are applied on the way to the final response values, but the discussion of the respective details is out of the scope of this document.

2. Instrument Response Calibration

In order to establish a relation between the measured intensities (Rayleigh channel) or the fringe position (Mie channel) and the frequency of the backscattered light, a calibration procedure is required. The Aeolus-specific Instrument Response Calibration (IRC) is performed with 40 frequency steps of 25 MHz each, hence, covering a range of 1 GHz around the operational laser frequency used for wind measurements. One frequency step comprises 2 so-called observations lasting 12 s each, which results in a duration of 16 min. Based on a satellite speed of 7.7 km/s the ground track length of an IRC extends to almost 7400 km.

During an IRC the influence of the wind speed needs to be excluded. Therefore, the Aeolus satellite is rotated into a nadir-pointing attitude and the vertical component of the wind along the track is neglected, which is a reasonable assumption for polar regions with their lack of strong convection. Another argument for placing the IRCs over the Arctic or Antarctica is the high albedo of ice and snow in the UV, that leads to high signal-to-noise ratios for the ground returns. The availability and high quality of ground returns is particularly important to obtain a Mie response calibration

curve for the atmospheric path and to measure the relative velocity of the solid earth surface, whose expected value is 0 m/s.

From the beginning the IRC was seen as a crucial contribution to the strategy for the correction of instrumental drifts throughout the mission lifetime. This strategy also included the spectral characterization of the instrument using internal measurements and the use of ground-return velocities for the correction of remaining linear and harmonic biases in the wind speed. Consequently, considerable effort had been put into an End-to-End simulator, but also into the ALADIN Airborne Demonstrator already before launch of the satellite, when several ground-based and airborne campaigns were conducted to investigate the overall performance of such a wind lidar system, to validate the measurement principle and to optimize the retrieval algorithms [6,7].

A total of 133 IRCs were performed during the mission lifetime, of which 36 were with laser FM-A from launch until the end of June 2019, 85 with laser FM-B between July 2019 and September 2022, and 12 again with laser FM-A between November 2022 and March 2023.

In the following, the evaluation of IRCs is discussed exemplarily along IRC #016, which was conducted on 17 December 2018 with laser FM-A and reprocessed during preparation activities of the 4th Aeolus reprocessing campaign in 2024. It is one of the best performing IRCs regarding the ground visibility and the number of valid ground returns.

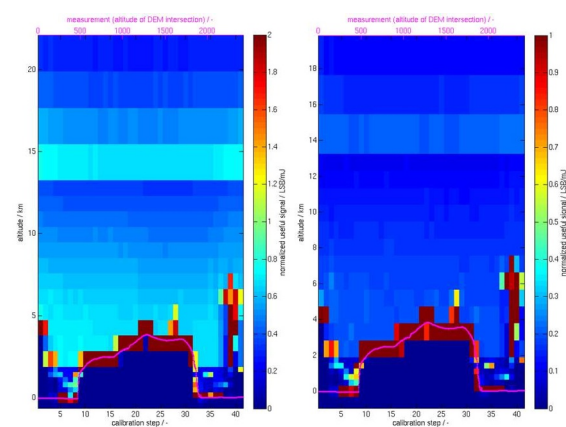


Figure 1. Rayleigh (left) and Mie (right) normalized useful signal from IRC #016.

Figure 1 shows the normalized (to laser emit energy) Rayleigh and Mie useful signals in units of LSB/mJ (LSB = least significant bit) per frequency step. The ground track starts

south of New Zealand, crosses Antarctica and ends in the Southern Atlantic. The high signals (dark red) that follow the Digital Elevation Model (DEM, pink) are considered as ground returns. Features with enhanced signal deviating from the DEM are considered as clouds or aerosol. The signal jump at 14 km and 15 km in the Mie and Rayleigh channel, respectively, is caused by an increase in the integration time, i.e. the range-gate thickness from 0.95 km to 2.21 km.

For the Mie channel two calibration curves are derived, one for the internal reference (signal not shown in Figure 1) and one for the ground returns. The same holds for the Rayleigh channel, but here an additional curve is derived from the molecular return signal of the atmosphere. To avoid contamination by ground, clouds or aerosol, only range-gates above 6 km altitude are considered and quality control is applied per bin by using a threshold on the scattering ratio.

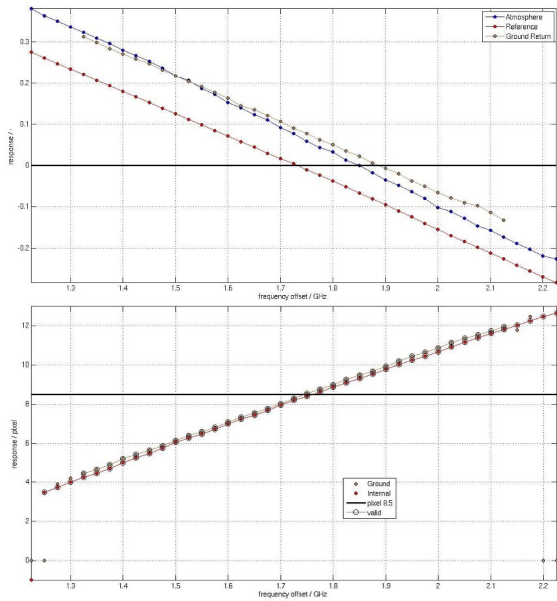


Figure 2. Rayleigh (top) and Mie (left) response calibration curves for the internal reference (red), the atmospheric return (blue) and the ground return (brown) of IRC #016.

The resulting response curves are presented in Figure 2. All frequency steps of the Rayleigh channel are valid for the internal reference and the atmospheric return, whereas several steps were removed for the ground return due to shadowing effects of the clouds visible at the start and end of the IRC in Figure 1. The same holds for the ground return in the Mie channel with 8 invalid steps, 4 on each side.

By linearly fitting these response curves, one obtains the slope, the intercept (intersection point with y-axis) and the offset frequency (intersection point with x-axis). The values for these parameters derived from IRC #016 are listed in Table 1 and are typical for the first period laser FM-A operation.

Table 1. Calibration curve properties

Rayleigh			
	Slope / 1/GHz	Intercept / -	Offset freq. / GHz
Refer.	-0.559	0.963	1.725
Atmos.	-0.623	1.150	1.847
Ground	-0.557	1.053	1.889
Mie			
	Slope / pixel/GHz	Intercept / pixel	Offset freq. / GHz
Refer.	9.468	-8.241	0.870
Ground	9.482	-8.095	0.854

Obviously, for both Mie and Rayleigh channel, the response curves of the ground and the internal reference remarkably differ in terms of the intercept, although both signals are very similar, i.e. spectrally narrow compared to the atmospheric return. This difference varies with time and can be traced back to different illumination conditions of the interferometers on these two optical paths [8]. It is important to note that slope and intercept values are the only IRC-related LIB information forwarded to the L2B processor, whose wind retrieval is additionally based on a method using another type of internal reference calibration data [9].

The IRC measurements have shown a non-linear dependency between the frequency Doppler shift and the Mie and Rayleigh response, respectively. In order to take these deviations into account and to reduce the systematic and random error on the wind speeds, the wind retrieval algorithm involves a non-linearity array for the Mie channel as well as a polynomial fit of 5th order for the Rayleigh response curve:

$$R_R(f) = \sum_{i=0}^5 (c_i + f^i) \quad (2)$$

As instrumental drifts can be induced, for example, by slowly changing incidence angles of the light onto the spectrometers, IRCs are not only used for calibration of Level-1B winds, but also for monitoring the health of the involved parts of the system.

3. Refinement of the calibration approach based on real data

Following the launch of Aeolus, unexpected and varying biases in wind speed were observed. These biases could not be effectively addressed using existing methods such as the IRCs. A new correction method was introduced to the L2B wind processor, taking into account temperature gradients across Aeolus' primary telescope mirror [10].

Additionally, comparisons of Aeolus winds against winds from the European Centre for Medium-Range Weather Forecasts revealed systematic errors in the Mie channel winds, indicating imperfect calibration data [11].

Following a temporary suspension of IRCs in February 2020, a new calibration mode was implemented: Instrument Response Off-Nadir Calibration (IRONIC). With a similar setup of the actual procedure but performed under the 35° off-nadir pointing, IRONICs were thought to partly take over the role of IRCs. However, the characteristics of the response curves of both modes differ slightly but systematically, which can be attributed most likely to different temperature environments under the different viewing angles. This raises the question whether or not IRCs in the implemented form are actually suitable for deriving wind speed with low systematic error, considering the mission requirement of a maximum bias of 0.7 m/s on horizontal LOS winds [12].

Consequently, one focus during the preparation of the upcoming Aeolus-2 mission is on improving the thermal stability of the satellite structure, the telescope, the lasers and the receivers in combination with a refined method for the instrument response calibration taking into account the lessons-learned from Aeolus.

4. Acknowledgements

This work was supported by ESA under the Aeolus DISC contract no. 40000126336/18/I-BG and 4000144330/24/I-AG.

5. References

[1] European Space Agency ESA, 2008: ADM-Aeolus Science Report, ESA SP-1311, 121 pp.
[2] O. Reitebuch, O., 2012: The space-borne wind lidar mission ADM-Aeolus. in Atmospheric Physics – Background, Methods, Trends. U. Schumann (Ed.) Springer Series on Research Topics in Aerospace, 815-827.

[3] O. Reitebuch, C. Lemmerz, O. Lux, U. Marksteiner, S. Rahm, F. Weiler, B. Witschas, M. Meringer, K. Schmidt, D. Huber, I. Nikolaus, A. Geiss, M. Vaughan, A. Dabas, T. Flament, H. Stieglitz, L. Isaksen, M. Rennie, J. de Kloe, G.-J. Marseille, A. Stoffelen, D. Wernham, T. Kanitz, A.-G. Straume, T. Fehr, J. von Bismarck, R. Floberghagen, T. Parrinello, „Initial assessment of the performance of the first wind lidar in space on Aeolus“, 29th Int. Laser Radar Conference ILRC, June 24-28, 2019 Hefei, China, EPJ Web Conferences 237, 01010 (2020).
[4] M. Rennie, L. Isaksen, F. Weiler, J. de Kloe, T. Kanitz, O. Reitebuch, “The impact of Aeolus wind retrievals on ECMWF global weather forecasts”, QJRMS, Volume 147, Issue 740, pp. 3555-3586, (2021).
[5] O. Lux, D. Wernham, P. Bravetti, P. McGoldrick, O. Lecrenier, W. Riede, A. D’Ottavi, V. De Sanctis, M. Schillinger, J. Lochard, J. Marshall, C. Lemmerz, F. Weiler, L. Mondin, A. Ciapponi, T. Kanitz, A. Elfving, T. Parrinello, and O. Reitebuch, “High-power and frequency-stable ultraviolet laser performance in space for the wind lidar on Aeolus”, Optics Letters, Vol. 45, Iss. 6, pp. 1443-1446, (2020).
[6] U. Marksteiner, “Airborne Wind Lidar Observations for the Validation of the ADM-Aeolus Instrument”, Ph.D. Thesis, Technical University Munich, (2013).
[7] U. Marksteiner, C. Lemmerz, O. Lux, S. Rahm, A. Schäfler, B. Witschas and O. Reitebuch, “Calibrations and Wind Observations of an Airborne Direct-Detection Wind LiDAR Supporting ESA’s Aeolus Mission”, Remote Sensing, 10(12), 2056 (2018).
[8] U. Marksteiner, O. Lux, O. Reitebuch, J. de Kloe, G.-J. Marseille and M. Rennie, “Overview of Instrument Response Calibrations”, Aeolus Science Conference, 22-26 May 2023, Rhodes, Greece, (2023).
[9] A. Dabas, M. L. Denneulin, P. Flamant, C. Loth, A. Garnier, and A. Dolfi-Bouteyre, “Correcting winds measured with a Rayleigh Doppler lidar from pressure and temperature effects”. Tellus A, 60(2):206-215, (2008).
[10] F. Weiler, M. Rennie, T. Kanitz, L. Isaksen, E. Checa, J. de Kloe, N. Okunde, O. Reitebuch, “Correction of wind bias for the lidar on-board Aeolus using telescope temperatures”. AMT, 14, 7167–7185, (2021).
[11] G.-J. Marseille, J. de Kloe, U. Marksteiner, O. Reitebuch, M. Rennie and S. de Haan, “NWP calibration applied to Aeolus Mie channel winds”, Q. J. Roy. Meteorol. Soc., Vol. 148, 1020-1034, (2022).
[12] ESA, “ADM-Aeolus Mission Requirements Document”, AE-RP-ESA-SY-001, Iss. 2, (2016).